Coastal flood risks in China through the 21st century – An application of DIVA

Jiayi Fang[1,2,3], Daniel Lincke[4], Sally Brown[3,5], Robert J. Nicholls[3,6], Claudia Wolff[7], Jan-Ludolf Merkens[7], Jochen Hinkel[4,8], Athanasios T. Vafeidis[7], Peijun Shi[2,9*], Min Liu[1]

1. Key Laboratory of Geographic Information Science, Ministry of Education, School of Geographic Sciences, East China Normal University, Shanghai 200241, China
2. Academy of Disaster Reduction and Emergency Management, Ministry of Emergency Management & Ministry of Education, Beijing 100875, China
3. School of Engineering, University of Southampton, Highfield Campus, Southampton, SO17 1BJ, UK
4. Global Climate Forum, 10178 Berlin, Germany
5. Department of Life and Environmental Sciences, Bournemouth University, Fern Barrow, Bournemouth. BH12 5BB. UK
6. Tyndall Centre for Climate Change Research, University of East Anglia, Norwich Research Park, Norwich NR4 7TJ
7. Coastal Risks and Sea-Level Rise Research Group, Department of Geography, Christian-Albrechts-University Kiel, Kiel, Germany
8. Division of Resource Economics, Albrecht Daniel Thaer-Institute and Berlin Workshop in Institutional Analysis of Social-Ecological Systems (WINS), Humboldt-University, 10099 Berlin, Germany
9. School of Geographical Science, Qinghai Normal University, Xining 810016, China

*Corresponding author: Prof. Peijun Shi (E-mail: spj@bnu.edu.cn)

Abbreviations

AW3D30: ALOS Global Digital Surface Model World 3D—30 m

DEM: Digital Elevation Model

DIVA: Dynamic Interactive Vulnerability Assessment

ESL: Extreme sea level

GADM: Global Administrative Areas

GCM: General Circulation Model

GDP: Gross Domestic Product

GPCN: Grid Population Dataset of China

GTSR: Global Tide and Surge Reanalysis

LECZ: Low Elevation Coastal Zone

RCP: Representative Concentration Pathways

SLR: Sea level rise

SSP: Shared Socioeconomic Pathways

Abstract

China experiences frequent coastal flooding, with nearly US$ 77 billion of direct economic losses and over 7,000 fatalities reported from 1989 to 2014. Flood damages are likely to grow due to climate change induced sea-level rise and increasing exposure if no further adaptation measures are taken. This paper quantifies potential damage and adaptation costs of coastal flooding in China over the 21st Century, including the effects of sea-level rise. It develops and utilises a new, detailed coastal database of China developed within the Dynamic Interactive Vulnerability Assessment (DIVA) model framework. The refined database provides a more realistic spatial representation of coasts, with more than 2,700 coastal segments, covering 28,966 km of coastline. Over 50% of China's coast is artificial, representing defended coast and/or claimed land. Coastal flood damage and adaptation costs for China are assessed for different Representative Concentration Pathway (RCP) and Shared Socio-economic Pathways (SSP) combinations representing climate change and socio-economic change and two adaptation strategies: no upgrade of currently existing defences and maintaining current protection levels. By 2100, 0.7-20.0 million people may be flooded/yr and US$ 67-3,308 billion damages/yr are projected without upgrade to defences. In contrast, maintaining the current protection level would reduce those numbers to 0.2-0.4 million people flooded/yr and US$ 22-60 billion/yr flood costs by 2100, with a protection investment costs of US$ 8-17 billion/yr. In 2100, maintaining current protection levels, dikes costs are two orders of magnitude smaller than flood costs across all scenarios, even without accounting for indirect damages. This research improves on earlier

national assessments of China by generating a wider range of projections, based on improved datasets. The information delivered in this study will help governments, policy-makers, insurance companies and local communities in China understand risks and design appropriate strategies to adapt to increasing coastal flood risk in an uncertain world.

Keywords: Coastal flooding, sea level rise, risk assessment, climate change impacts, China

1 Introduction

Coastal areas are threatened by extreme weather events and climate change. Coastal floods caused by extreme sea levels (ESLs) due to combined high tide and storm surges are one of the most serious risks, which impact upon society, the economy and the wider natural environment. Sea level rise (SLR) further exacerbates this risk over time (Nicholls, 2004; Hanson et al., 2011; Hallegatte et al., 2013; Nicholls et al., 2014; Hinkel et al., 2014).

Coastal areas in China are important population and economic centres and are prone to natural disasters, especially for flood disasters (Hu et al., 2018). Coastal China comprises 14 provincial-level administrative regions which encompasses a wide latitudinal range from Liaodong Bay (at 41° N) to the South China Sea (at 4° N), including one autonomous region: Guangxi; two municipalities: Shanghai and Tianjin; three Special Administrative Region: Taiwan, Hong Kong and Macao; eight provinces from north to south: Liaoning, Hebei, Shandong, Jiangsu, Zhejiang, Fujian, Guangdong

and Hainan. More than 40% of the population lives in coastal provincial administrative regions, which contribute nearly 60% of the national gross domestic product (GDP). About 47% of the national capital stock was found in the Eastern Economic Region[1] in 2012 (Wu et al. 2014). Coastal population and assets in China are growing much faster than in inland areas (Seto, 2011). It is expected that this trend and related coastal infrastructure development and maritime activities will continue with the proposal of China's 21st Century Maritime Silk Road programme (Liu, 2014). However, these areas also experience frequent storm surges and coastal flooding which caused approximately US$ 77 billion direct economic losses and more than 7,000 fatalities from 1989 to 2014 (Fang et al., 2017). Additionally, rapid urbanization has led to a sharp increase of exposure in coastal areas in China and has been accompanied by groundwater pumping causing subsidence, plus an expanding impermeable urban area. These risks are likely to grow due to climate change and increasing exposure if no further adaptation measures are taken.

Given this situation, it is crucial to analyse the future impacts of coastal flooding in China under a range of sea-level rise and socio-economic change scenarios; and also consider how adaptation could alter these impacts. This information will inform the long-term planning of development of the coastal zone of China. To our knowledge, a number of studies have considered sea-level rise in China (e.g., Han et al., 1995), or sea-level rise in parts of China (e.g., Wang et al., 1995; Huang et al., 2004; Kang et al.,

[1]Eastern Economic Region consists of Hebei, Beijing, Tianjin, Shandong, Jiangsu, Shanghai, Zhejiang, Fujian, Guangdong and Hainan. Except Beijing, other are coastal provincial administrative regions.

2016; Wang et al., 2018), but there is no quantitative national coastal flood impact assessment. This paper fills this gap by including improved coastal datasets and considering demographic and economic scenarios and coastal protection strategies.

The aim of this study is to investigate the coastal flood damage and adaptation costs across China by considering three Representative Concentration Pathways (RCP) and Shared Socio-economic Pathways (SSP) combinations representing climate change and socio-economic change, respectively, as well as considering two adaptation strategies. This is achieved by two objectives: 1) to generate a new and high-resolution coastal database for China; and 2) to assess potential coastal flood risks under the different scenarios and adaptation strategies.

Hinkel et al. (2014) conducted a global assessment of coastal flood risk, including China, using the Dynamic Interactive Vulnerability Assessment (DIVA) modelling framework. The original DIVA database was developed for global assessment (Vafeidis et al., 2008), and includes 226 segments covering 12,288 km of coastline in China. The official coastal length in China is about 18,000 km for the continental coast (Wang, 1980). A major constraint on coastal flood risk assessment at national scale is the data availability and quality (Nicholls et al., 2008). Therefore, when new datasets emerge, it is important to make the most of these in future analysis. For example, Wolff et al. (2016) suggest that a more refined segmentation using updated data within the DIVA modelling framework can improve coastal flood risk assessment. Hence, a new and more detailed coastal database is developed for China and linked to the DIVA algorithms for a national assessment.

126 The paper is structured as follows. Section 2 describes materials and methods used to
127 build the new and high-resolution coastal database of China. Section 3 shows the results
128 and discussion of coastal flood risk by considering various dimensions. Conclusions
129 are presented in Section 4.

130 2 Materials and methods

131 We use the DIVA coastal flooding module, as presented in Hinkel et al. (2014), to
132 calculate coastal flood risks in China. DIVA is an integrated, state-of the-art research
133 model of coastal systems that assesses biophysical and socio-economic consequences
134 of sea-level rise, socio-economic development and adaptation (Hinkel and Klein, 2009).
135 Changes in sea-level are represented by the RCPs (van Vuuren et al., 2011). In this case,
136 regional sea-level rise scenarios were used. Future coastal population exposure changes
137 are computed from SSPs (IIASA, 2012; O'Neill et al., 2014). Adaptation is an explicit
138 element of the DIVA framework. Within DIVA, the algorithms and database are
139 separated, where the latter is based on a linear segmentation of the coast (Vafeidis et
140 al., 2008).

141 Figure 1 summarises the methodology, which consists of three main steps. The first
142 step is to improve the quality and resolution of the spatial assessment units by using a
143 more detailed coastline and segmentation process (as discussed in Section 2.1). The
144 second step is to calculate exposure using elevation and population datasets, and to
145 create a data structure that enables the model to run (see Section 2.2). Last, the DIVA

coastal flooding module is used to assess future coastal flood risks for different scenarios and adaptation strategies (see Section 2.3).

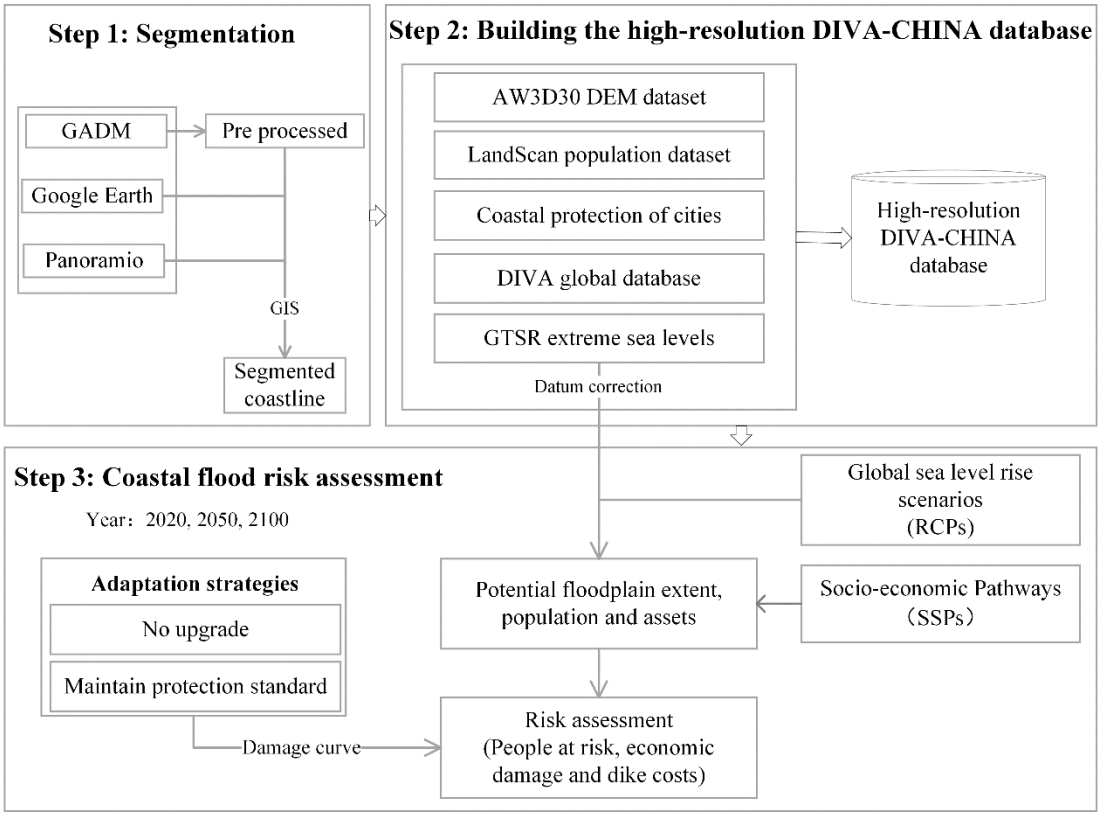

Fig. 1 Flowchart showing the general methodological approach by dividing into three steps.

2.1 Segmentation

The DIVA model operates on data attributed to coastline segments. As the resolution of the Chinese coastline in the global database is rather coarse, a refined version was developed for this study. To downscale the segmentation and the coastal database for China, we generated a larger number of segments and populated the database with local-level datasets, following similar approaches to those used in McFadden et al. (2007) and Wolff et al. (2016; 2018) (Supplementary Fig. S1). Each segment associated with a range of geophysical, ecology, economic and demographic information, reflects

159 a uniform changing response or sequence of responses within the coastal system, and
160 subsequent modelling and analysis are based on these segments.

161 The coastline acts as a base layer for all the following steps and hence plays a
162 fundamental role in the analysis. After reviewing several possible coastlines, we
163 selected the coastline from Global Administrative Areas (GADM) (Supplementary Tab.
164 S1) and pre-processed and transformed the data following Wolff et al. (2018). Then
165 urban and rural coasts have been identified based on the interpretation of satellite
166 imagery and an urban extent dataset (Huang et al., 2015; Xu et al., 2016). Urban areas
167 are defined with a predominantly impervious surface environment, such as buildings
168 and roads. Classification were based on visual interpretation of Google imagery and
169 urban extent dataset. Due to the lack of a national coastal geomorphic characteristics
170 dataset for coastal China, an independent consistent dataset was generated with Google
171 Earth and photos from the web-service "Panoramio" (http://www.panoramio.com/).
172 Panoramio provides location-tagged photographs for the whole study area and gave a
173 good impression of the type of coast, which has been used to monitor changes of
174 coastlines as an assistant tool (Scheffers et al., 2012). The geomorphic coastal type data
175 was then compiled based on the visual inspection from the available satellite imagery
176 as well as geographically tagged photos. Adjusted from Wolff et al. (2016), in this study,
177 the coastlines were classified into five main types: 1) sandy, 2) rocky (unerodible or
178 limited erodible), 3) muddy, 4) artificial and 5) river mouth (Supplementary Tab. S2).
179 Using this as a base layer, the coastline segmentation was performed within a GIS. The

coastline was split every time the type of coast differed based on the satellite data and photographs or a political boundary was crossed.

2.2 Building the high-resolution DIVA-China database

To build the refined database, we recalculate exposure at different elevation increments using baseline elevation and population datasets; we also update coastal protection data, extreme sea levels as well as parameters from the DIVA global dataset.

To assess coastal exposure to inundation, the bathtub approach is employed, which is widely used for macro-scale analysis (e.g. Kebede et al., 2012; Hallegatte et al., 2013). The hydrological connectivity (8 neighbour cells) is also considered when calculating the inundated area within the bathtub approach (Li et al., 2009). The free-downloaded Digital Elevation Models (DEMs) ALOS Global Digital Surface Model (ALOS World 3D—30 m, AW3D30 for short) is employed. AW3D30 with a spatial resolution of 1 arcsec (approx. 30 m) and a vertical resolution of 1 m (Tadono et al., 2016). The dataset is published based on the global digital surface model dataset (5-meter mesh version) of the 'World 3D Topographic Data' which is one of the most precise global-scale elevation datasets at this time (Courtya et al., 2017; Hu et al., 2017). The population count datasets of LandScan have been used to calculate the exposed population. The dataset is with a resolution of 30 arcsec (approx.1 km) and is with base year of 2010 (Bright et al., 2011).

There is no empirical data on actual protection levels of China in the global DIVA database. Thus, we use flood protection data of coastal cities in China from various sources (Supplementary Tab. S3). This table provides flood protection standard by

return period. For those coastal cities without protection data, we follow the National Standard for Flood Control of China (2014) to estimate the flood protection standard. The standard requires that cities with permanent resident population of more than 1.5 million people are equipped with at least 200-year return period flood protection facilities (Supplementary Tab. S4). The protection information is attached to the segments of those population centres that have been identified in the segmentation.

Extreme water levels given for different return periods utilised in this study are from the first global reanalysis of storm surges and extreme sea levels (GTSR) based on hydrodynamic modelling (Muis et al., 2016). GTSR consists of time series of tides and surges, and estimates of extreme sea levels. The extreme water levels have been datum corrected to the same datum as the DEM used in DIVA.

Other basic information used in DIVA (e.g. GDP per capita of China) has been updated from the base year of 1995 to a baseline in 2010. For example, based on recent coastal projects construction in China, the cost of seawall construction was US$3.4 million/km/m (Ke, 2014). The DIVA database for China is compiled by using similar approaches which can be found in Vafeidis et al. (2008).

2.3 Coastal flood risk assessment

The coastal flooding module in DIVA (version 5.0.0) was used to assess coastal flood risks in China. Local relative sea-level change is computed by adding regionalised climate-induced sea-level rise scenarios with glacial isostatic adjustment data (Peltier,2000). In addition, for segments located in river deltas a subsidence rate of 2 mm/yr was assumed (following Hinkel et al., 2014).

Population and assets exposure to coastal flood events are computed using cumulative population and asset exposure functions. The estimation of the value of assets on a given elevation increment is undertaken by multiplying the population count with the local GDP per capita (province level) and an empirically estimated GDP-to-assets ratio of 2.8 taken from Hallegatte et al. (2013). We assume that when the water level is below the protection standard, people and assets are protected, and thus the loss is zero. For people, if there is no protection or the extreme water level is higher than the protection standard, the damage function is identical to the cumulative exposure function. In contrast for assets we assume a logistic depth-damage function (giving the fraction of assets damaged for a given flood depth) with a 2-m flood destroying 50% of the assets (Messner et al., 2007; Yin et al., 2012; Fig. 2). A more detailed description of the coastal flooding module in this study is presented in Hinkel et al. (2014).

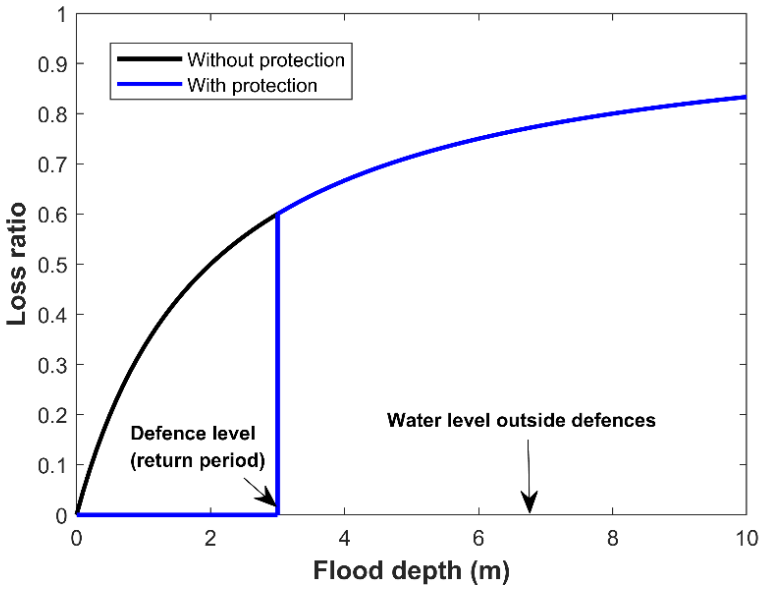

Fig. 2 Damage curve for the assessment of assets in the DIVA flood module (Blue line shows an example of a 3 m of defence, the loss ratio over 3 m is same as without protection).

The following parameters of coastal flooding are analysed in this study:

1) Exposure of the 100-year return period flood event: floodplain area extent (km^2), exposed population (million) and assets (billion US$) (ignoring dikes);
2) Expected number of people flooded per year (million/yr);
3) Expected average annual flood costs (in billion US$/yr);
4) Expected average annual dike costs comprise capital costs of building and upgrading dikes, as well as dike maintenance costs (in billion US$/yr).

Adaptation is modelled by dikes, which is consistent with current practice in China where dikes are widely used (Ma et al., 2014). There are two protection strategies: (1) maintain protection standard (2010), and (2) no upgrade of currently existing defences. Maintain protection standard means that dikes are kept at the current protection standard and thus raised over time with relative sea-level rise to against same degree of ESL. No upgrade means that dikes are kept at 2010 heights and not raised and thus become increasingly less effective as sea levels rise. The protection standard does not change, even if socio-economic conditions change.

Future potential impacts in DIVA are assessed by taking sea-level rise and socioeconomic development scenarios into account. Following the work of Hinkel et al (2014), we used sea-level rise scenarios derived from three RCPs (RCP2.6, 4.5, and 8.5), four general circulation models (GCMs) (HadGEM2-ES, IPSL-CM5A-LR, MIROC-ESM-CHEM, and NorESM1-M) and three land-ice scenarios (low, medium and high). A more detailed description of these sea-level rise scenarios can be found in Hinkel et al. (2014). The projected relative sea-level rise along coastal China at the end of this century ranges from 21 cm to 119 cm with respect to the 1985-2005 mean across

all GCMs and emission scenarios. The median value in 2100 for RCP2.6 is 38 cm, for RCP4.5 55 cm and for RCP8.5 85 cm (Fig. 3a; Supplementary Tab. S5).

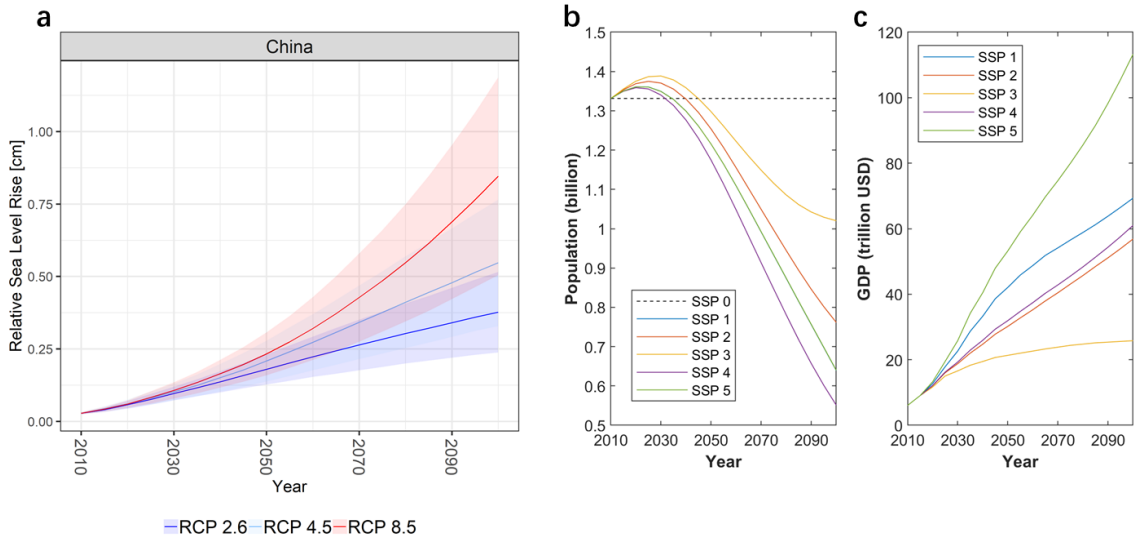

Fig. 3 a) The mean relative sea-level rise for China under sea-level rise scenarios (reference period: 1985-2005; Lines refer to median values, and shades areas show ranges of maximum and minimum values); b) Population (SSP5 overlays SSP1 for population, SSP0 only refers to no change of population); c) GDP of China for socio-economic scenarios from 2010 to 2100.

We utilise the SSPs to account for socioeconomic development. The SSPs provide five pathways of socioeconomic development (SSPs 1-5) including projections on population (Samir, K.C. and Lutz, W., 2017) and GDP (Leimbach et al., 2017). For this study, we assume homogeneous growth patterns and apply the national projections of population and GDP under each SSP to the segment to calculate future exposure. According to mean global total fertility rate, China is a low-fertility country (Samir and Lutz, 2017). SSP1 assumes sustainable development with emphasis on education, medical service and renewables, low fertility, low mortality and medium migration; SSP2 is moderate development, with medium fertility, mortality and migration. SSP3

281 is with high population growth and mortality, as well as low migration. SSP4 indicates
282 low fertility and high mortality. In the SSP5 storyline, there is rapid economic
283 development heavily based on fossil-fuel, with low capacity in the mitigation
284 challenges (Samir and Lutz, 2014). Thus, the population projections for China will
285 increase from 2010 to 2030, peaking at nearly 1.4 billion populations, then decreasing
286 until the end of this century across all five SSPs scenarios (Fig. 3b). The trajectories are
287 similar for the five SSPs until around 2030. Substantial difference occurs after then,
288 with highest population in SSP3 (~1.0 billion) and the lowest in SSP4 (~0.6 billion) in
289 2100. As population decline in China is significant in all scenarios, an additional set of
290 runs with constant (2010) population (SSP0) is included to demonstrate the changes
291 due to climate change without demographic changes. The population of SSP0 is higher
292 than the other five SSPs after 2035. The GDP increases for the five SSP scenarios until
293 2100. The highest GDP is SSP5 (~US$113 trillion) and the lowest is SSP3 (~US$26
294 trillion) (Fig. 3b) in 2100.

295 Based upon the three RCP scenarios and five SSP scenarios, we generate a 3 × 5 matrix
296 of core scenarios. We note that some RCP-SSP combinations (e.g., RCP2.6-SSP3) are
297 unlikely to arise in practice (van Vuuren and Carter, 2014). Three plausible SSP and
298 RCP combinations provide the basis for the analysis of future coastal flooding risks
299 here, namely, RCP2.6-SSP1, RCP4.5-SSP2, and RCP8.5-SSP5 (Vousdoukas et al.,
300 2018). RCP2.6-SSP1 describes a low greenhouse gas emission scenario and sustainable
301 development scenario. RCP4.5-SSP2 indicates a moderate development pathway with
302 moderate greenhouse gas emissions and development. RCP8.5-SSP5 refers to a world

with fossil-fuel based development. In order to quantify relative contribution of climate and population on exposure (as described in Section 3.2), we adopt the method from Jones et al. (2015) and Liao et al. (2019). We decompose the change of population exposure into three effects, i.e., climate effect, population effect and joint change effect.

$$\Delta \mathrm{E} = E_j - E_i = P_j \times C_j - P_i \times C_i = P_i \times \Delta \mathrm{C} + C_i \times \Delta \mathrm{P} + \Delta \mathrm{C} \times \Delta \mathrm{P} \quad (1)$$

To consider relative contribution of the factors compared with the population exposure in the base year, the percentage of the total change was considered (as used in Fig 6). This is noted in Equation 2, which was then multiplied by 100 to give a percentage.

$$\frac{\Delta \mathrm{E}}{E_1} = \frac{P_i \times \Delta \mathrm{C} + C_i \times \Delta \mathrm{P} + \Delta \mathrm{C} \times \Delta \mathrm{P}}{P_i \times C_i} = \frac{\Delta \mathrm{C}}{C_i} + \frac{\Delta \mathrm{P}}{P_i} + \frac{\Delta \mathrm{P} \Delta \mathrm{C}}{P_i C_i} \quad (2)$$

In this equations, ΔE is the total change in population exposure, E_i is population exposure in base year, E_j is population exposure in base year. C_i and P_i are exposed areas which is dominant by SLR and population in base year, C_j and P_j are exposed areas and population in target year, and ΔC and ΔP are the change in exposed areas which is dominant by SLR and population from base year to target year. Here we refer to $C_i \times \Delta P$ as the population effect, $P_i \times \Delta C$ as the climate effect and $\Delta C \times \Delta P$ as the joint change effect.

3 Results and discussion

3.1 DIVA-China database

The new Chinese coastline segmentation produces 2,760 variable-length segments with maximum segment length of 99.99 km and minimum length of 0.11 km. The average segment length is 10.50 km. Compared with the global DIVA database, this is a 10-fold

increase in the number of segments, which results in a 136% increase in coastline length from 12,288 km to 28,966 km (Tab. 1). The main reason for the increased coastline length is due to the inclusion of nearshore small islands (e.g. Zhoushan Islands in Zhejiang Province) (Supplementary Fig. S2), as previous studies were mainly based on continental coastlines.

The coastline of China has undergone rapid changes in the last 100 years due to natural factors (e.g. sediment supply) as well as anthropogenic influence (e.g. construction of dams in the catchments, dikes, land claim and other engineering structures) (Wang and Aubrey, 1987). Based on the high-resolution segmentation, rocky coast accounts for 9,577 km or 33% of the total coastline. It is mainly distributed in small islands of Liaodong Peninsula, Zhejiang, Fujian, Guangdong and Taiwan provinces. Zhejiang and Fujian have the longest rocky coasts, at 2135 and 2183 km including small islands, respectively, accounting for 35% and 43% of the total length of the province (Tab. 1).

Tab. 1 Length of China's coastline according to the coastal typology classification based on the high-resolution segmentation.

Coastal type	**Coastline (km)**	**Percent (%)**
Sandy	2703	9.3
Rocky	9577	33.0
Muddy	1722	6.0
Artificial coasts	14828	51.2
River mouth	137	0.5
Total	28967	100

Sandy coast constitutes about 2,703 km, or 9.3% of the country's coastline. It is mainly located in Hainan province with a length of 564 km or 34.0% of the province's coastline. Muddy coast accounts for 6.0% of the national coastline. The length of muddy coast identified in this study is significantly less than previous studies (Wang and Aubrey,

1987). The main reason is that muddy coasts have abundant resources, which are conducive to the development of aquaculture and reclamation for other industries. Given this and its high erosion potential, it has been protected and/or has been converted to artificial coast (Sun et al., 2015; Luo et al., 2015). The length of river mouths is about 137 km, which is consistent with the length of the estuaries and coasts obtained from other studies (e.g. Gao et al., 2013).

Tab. 2 Coastline, artificial coastline, areas and population in the low elevation coastal zone (LECZ) areas (DEM ≤ 10 m) in the first-level administrative divisions of China.

Province	Coastline (km)	Percent of national coast (%)	Artificial coastline (km)	Percentage of artificial coast to provincial coasts (%)	Territory (km^2)	Areas of LECZ (km^2)	LECZ to territory (%)	Total provincial population (million)	Population in LECZ (million)	Population in LECZ to total province (%)	Population density in LECZ (people/km^2)
						AW3D30			LandScan		
Liaoning	2620	9.1	1685	64.3	135,916	12,262	9.0	44.7	6.2	13.8	503
Hebei	376	1.3	307	81.6	176,101	17,663	10.0	71.5	7.8	10.9	442
Tianjin	125	0.4	123	98.7	10,985	9,866	89.8	10.6	9.4	88.6	949
Shandong	2838	9.8	1735	61.1	148,269	21,031	14.2	96.1	8.6	8.9	407
Jiangsu	1247	4.3	1177	94.4	99,227	66,532	67.1	78.1	51.5	65.9	774
Shanghai	635	2.2	631	99.4	6,811	6,458	94.8	17.7	14.7	83.4	2279
Zhejiang	6135	21.2	2287	37.3	103,621	16,005	15.4	49.0	21.9	44.7	1367
Fujian	5042	17.4	1923	38.1	127,161	3,540	2.8	36.4	6.8	18.7	1921
Guangdong	5344	18.5	2758	51.6	191,334	20,243	10.6	91.3	33.3	36.5	1646
Guangxi	1299	4.5	890	68.5	252,891	1,623	0.6	46.9	0.9	1.8	524
Hainan	1647	5.7	190	11.5	38,762	2,554	6.6	8.1	1.9	23.4	736
Hong Kong	653	2.3	483	74.0	1,229	186	15.1	7.0	1.4	19.7	7377
Macau	59	0.2	52	87.9	37	12	32.7	0.4	0.2	38.1	13291
Taiwan	947	3.3	586	61.9	103,621	2,942	2.8	23.0	4.6	20.1	1570
Total	28967	100	14828	51.2	1,395,966	180,916	13.0	580.8	169.2	29.1	934

Artificial coastline amounts to 14,828 km in China, which is more than half of the country's coastline (Tab. 2). The artificial coastlines in Tianjin, Jiangsu and Shanghai amount to more than 94% of the provincial coast. The lowest percentage of artificial coastline is Hainan Province covering only 11.5% its coasts. The utilization of the mainland coast in China has increased continuously and dramatically from the 1940s to today, driving the creation of artificial coasts (Wu et al., 2014; Wang et al., 2014). The main reasons for the high percentage of artificial coastlines in China are due to (1) massive land reclamation for the need of land supply (Hou et al., 2016), (2) construction of seawalls and embankments to protect erosion and flooding (Luo et al., 2015), (3) seaward artificial aquaculture which encloses many coastal areas, and (4) seaward artificial wetlands with dikes (Sun et al., 2015) (Supplementary Fig. S3). Extensive land reclamation has occurred in coastal China comprising 13,380 km^2 from 1950 to 2008 (Fu et al., 2010), especially in Tianjin, Hebei, Jiangsu and Shanghai. The decline of natural coasts and the high percentage of artificial coasts is similar to other studies (e.g. Gao et al., 2013; Hou et al., 2016).

After the segmentation, coastal protection standards along coastal China were extracted from Li et al. (2003), Aerts et al. (2009) and Hallegatte et al. (2013) (Fig. 4). Shanghai and Hong Kong have the highest protection level at 1000-year and 900-year return period, respectively. Tianjin and Taipei have 200-year return period. Coastal provincial capitals, such as Hangzhou (200-year) and Guangzhou (200-year), have higher protection standard than other coastal cities, such as Ningbo (100-year), Quanzhou (100-year) and Shenzhen (100-year) .

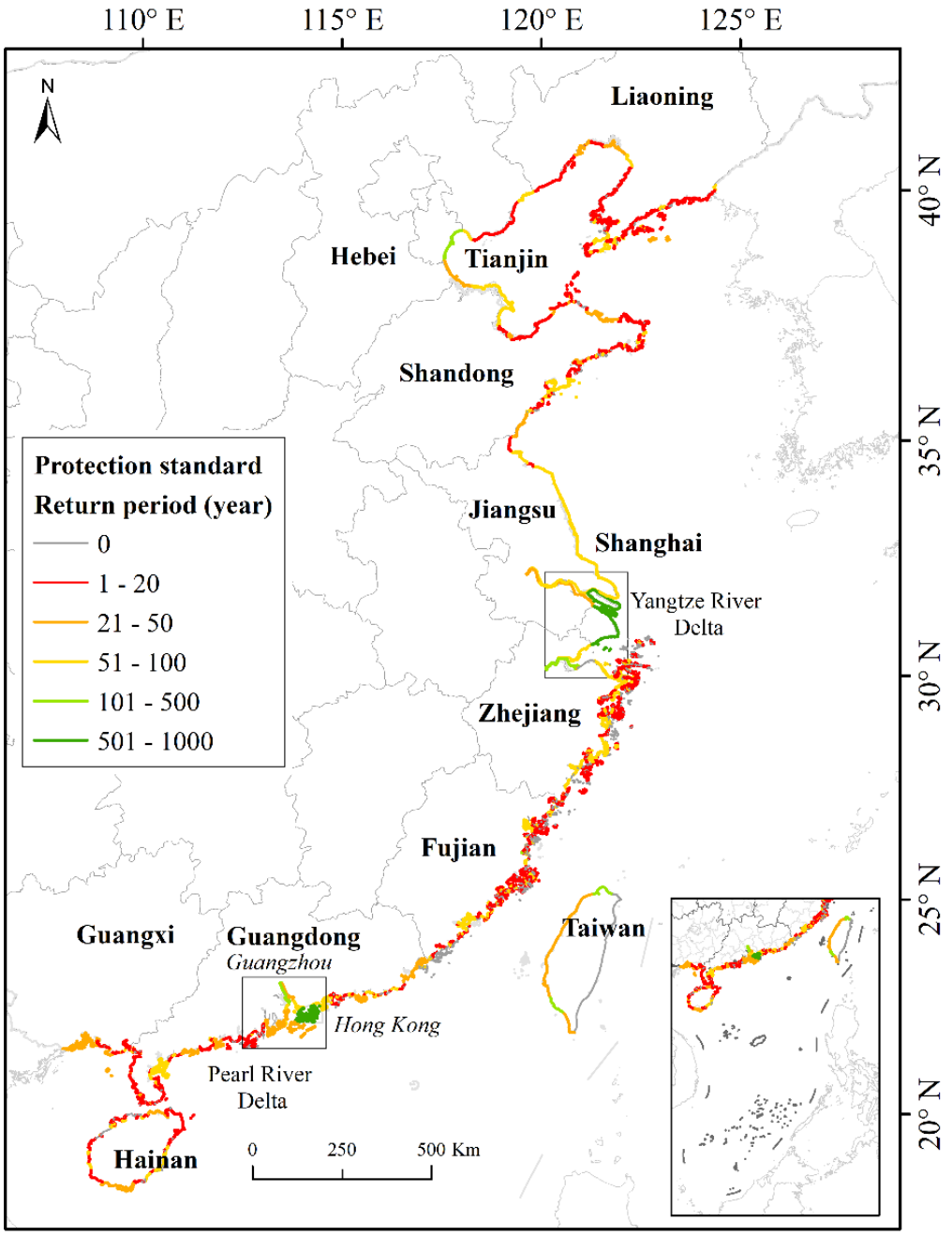

372

373 Fig. 4 Coastal protection standard (return period) of China.

374 According to the DIVA-China database, the total area of the low elevation coastal zone (LECZ,
375 defined as the contiguous area along the coast that is less than 10 m above the sea level) in
376 China is 180,916 km^2, which account for 13.0 % of coastal provincial territory (Tab. 2). Jiangsu
377 Province has the largest LECZ of 66,532 km^2, which accounts for 67.1 % of its territory and
378 more than one third of all LECZ in China (Supplementary Fig. S4). Shanghai and Tianjin, two

of the largest and most important ports in China, have the largest percentage of LECZ to its territory, at about 95 % and 90 %, respectively. The region with the lowest percentage of LECZ is Guangxi, with only 0.6 %.

The LECZ population is ~170 million. Similarly to the LECZ, Jiangsu Province has the largest LECZ population at 51.5 million, or nearly one third of the LECZ population in China (Supplementary Fig. S4), followed by Guangdong Province with 33.3 million. Both Tianjin and Shanghai have the highest percentage of population living in the LECZ, with 88.6 % and 83.4 %, respectively. Except for Macau, Guangxi has lowest population of 0.9 million living in LECZ, only accounting for 1.8 % of the total provincial population. Hong Kong and Macau have the highest LECZ population density in China. In Mainland China, Shanghai has the highest LECZ population density with 2,279 people per km^2. These findings are in the same range as the findings of McGranahan et al. (2007), Neumann et al. (2015) and Liu et al. (2015).

3.2 Exposure of the 100-year return period flood event

Using the high-resolution segmentation, we calculated exposed areas, population and assets (ignoring dikes) in the 100-year coastal floodplain (Fig 5). With SLR, areas below the 100-year floodplain rapidly increase. The 100-year floodplain area is approximately 49,000 km^2 (2020), growing to 53,000 (RCP2.6) to 74,000 km^2 (RCP8.5) by 2100. The SLR scenario of RCP8.5 under the MIROC-ESM-CHEN model, combined with high ice melting scenario, is the scenario with the highest relative sea level rise and the largest floodplain under all GCM-RCP-ice melting combinations. RCP2.6 under the NorESM1-M model, combined with a low ice melting scenario, is the lowest SLR scenario and the smallest flooded area. In this study, the area of the 100-year floodplain depends only on the SLR scenario, as we assume, following 20th century observations (Menendez and Woodworth, 2011), extreme water levels to increase uniformly with sea-level rise.

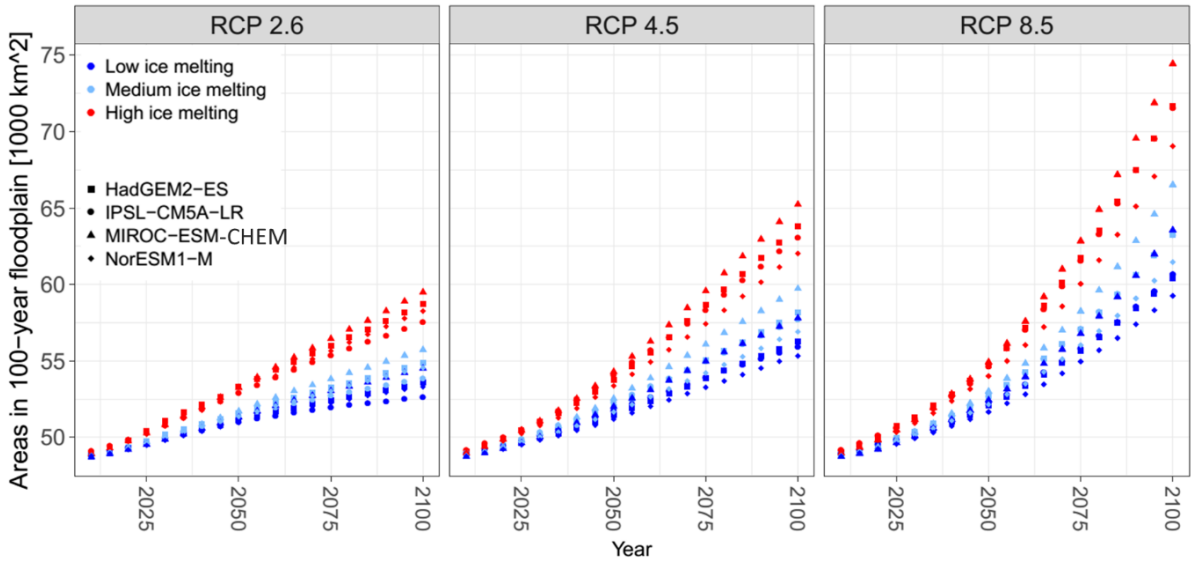

403

404 Fig. 5 Areas of the 100-year coastal floodplain over the 21st century under SLR scenarios.

405

406 The exposed population in SSP0 is lower compared with the other four SSPs before 2030
407 because of the assumption of no growth of population. After 2030, the exposed population
408 keeps increasing under SSP0, while they decrease under the other four SSPs due to the decline
409 of total population in these scenarios (Fig. 6a). Considering demographic changes and SLR,
410 the 100-year floodplain exposed population is 36.5 million (2020) people, changing to 18.1-
411 27.0 million (2100). Under RCP2.6-SSP1, RCP4.5-SSP2 and RCP8.5-SSP5, the exposed
412 population shows a decreasing trend after peaking around 2030 with the greatest decline in
413 RCP2.6-SSP1. To analyse the temporal change in exposure and relative contribution due to
414 climate, population and joint change effects, we calculate the annual relative contribution (Fig.
415 6b) as a percentage change, as defined in Eq.2. The sum of these is known as the total change.
416 Sea-level rise (climate effect) always leads to increasing population exposure in the 21st century.
417 Before 2030, exposed population is still increasing. The population change leads to increased
418 exposure at the beginning of this century but then leads to a reduction after 2040. The
419 population effect becomes more prominent than population and joint change effects, which

leads to the total decrease of exposed population. Thus, change in population exposure to coastal floods is mainly due to the population effect.

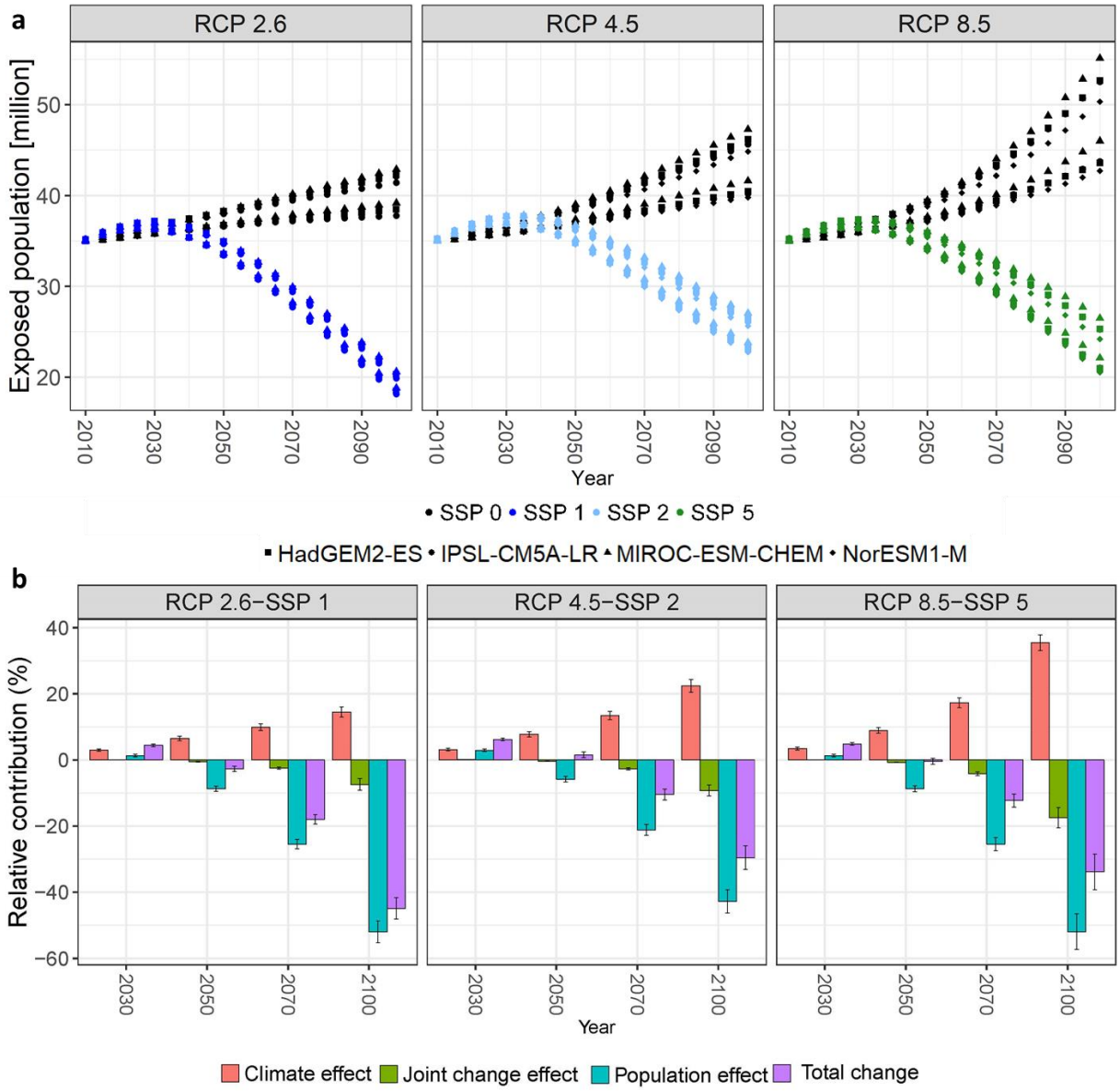

Fig. 6 a) Population below 100-year coastal floodplain under RCP-SSP scenarios in the 21st century; b) Relative contribution of changes to exposed population (below 100-year coastal floodplain) under SSP-RCP scenarios. Error bars illustrate the standard deviation in total exposure change across scenarios for each effect.

Considering demographic changes, the assets below 100-year floodplain are US$ 1.6 trillion (2020), which grows to US$ 4.5-11.1 trillion (2100). Exposed assets increases before 2050 in RCP2.6-SSP1, then begin to decline slightly. Except for the RCP2.6-SSP1, the effected assets

under the other three combination shows upward trends, with RCP8.5-SSP5 showing the highest increase.

3.3 Risks and adaptation costs

The expected number of people flooded annually is presented in Fig. 7a. Due to protection, the population flooded is much smaller than the exposed population. The expected number of people flooded annually is highest under RCP8.5-SSP5 and lowest in RCP2.6-SSP1. Flooded population grows slightly slower at the beginning of the century, increase slowly until 2050 (less than 0.25 m relative SLR), then accelerates faster, especially after 2070.

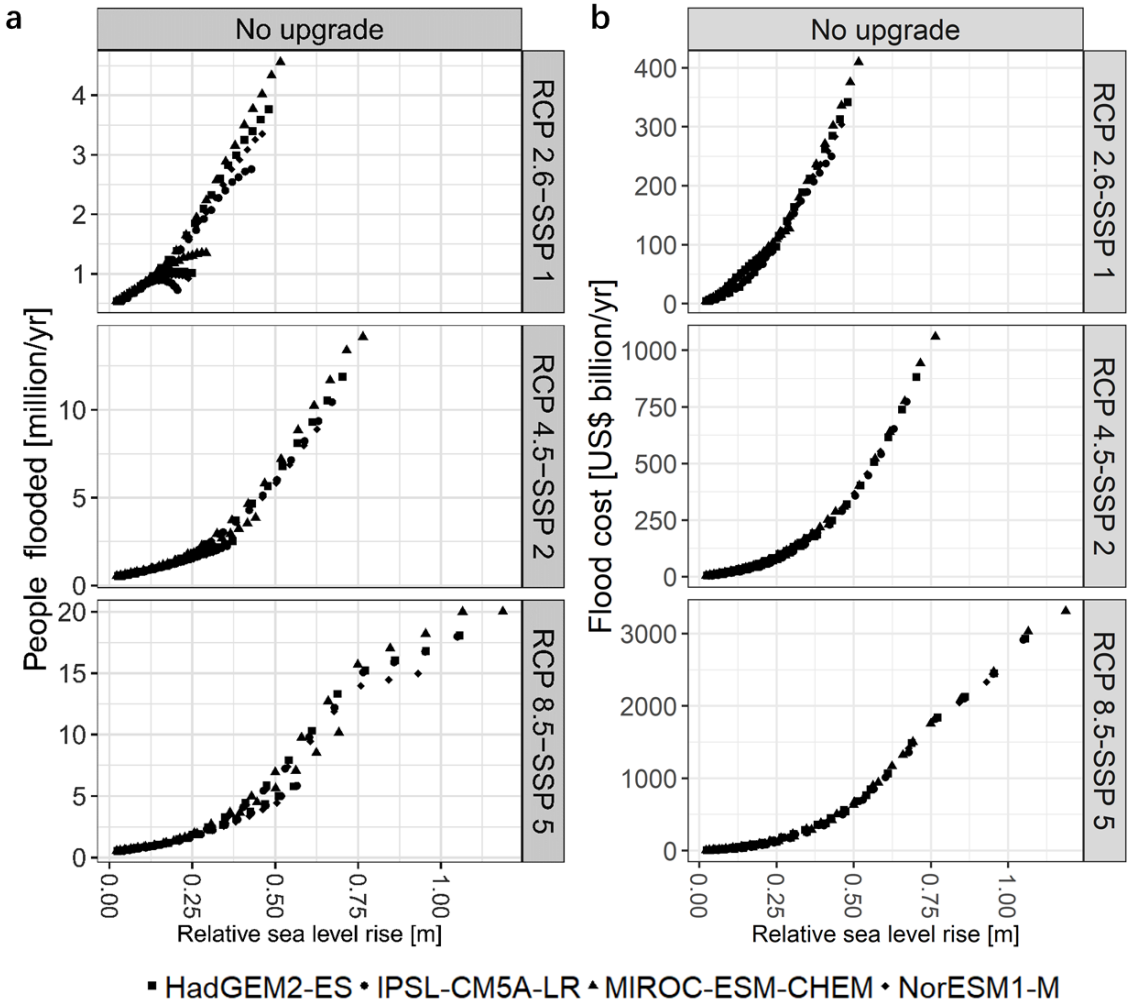

Fig. 7 People flooded and flood cost of China with relative sea level rise in the 21st century under a no upgrade to adaptation strategy with respect to 2010.

443 The number of people flooded per year is about 0.6 million in 2020, increasing to ~0.7 to 20
444 million people per year at end of this century if there is no upgrading to protection levels. This
445 number drops to 0.2 to 0.4 million with maintaining protection standard (Fig. 8). The change
446 of population flooded shows that the effect of adaptation strategy and declines of total
447 population exceeds the climate effect under the maintaining the constant protection. The lack
448 of update in protection and the climate effect lead to higher population exposure, even when
449 there are declines of total population. Hence, maintaining constant protection reduces impacts
450 by about one order of magnitude.

451 The flood costs are shown in Fig.7b. Flood costs are highest under RCP8.5-SSP5 and the lowest
452 under RCP2.6-SSP1. Flood costs grow slower at the beginning of the century, but then
453 accelerates faster reflecting an accelerating rise in sea-level. The average annual flood cost is
454 about US$ 10 billion per year in 2020. This increases by ~7–330 times to US$ 67-3,308 billion
455 per year by the end of 21st century under the most pessimistic scenario, with no upgrade. This
456 number drops to US$ 22-60 billion flood damage per year with maintaining constant protection
457 standards (Fig. 8).

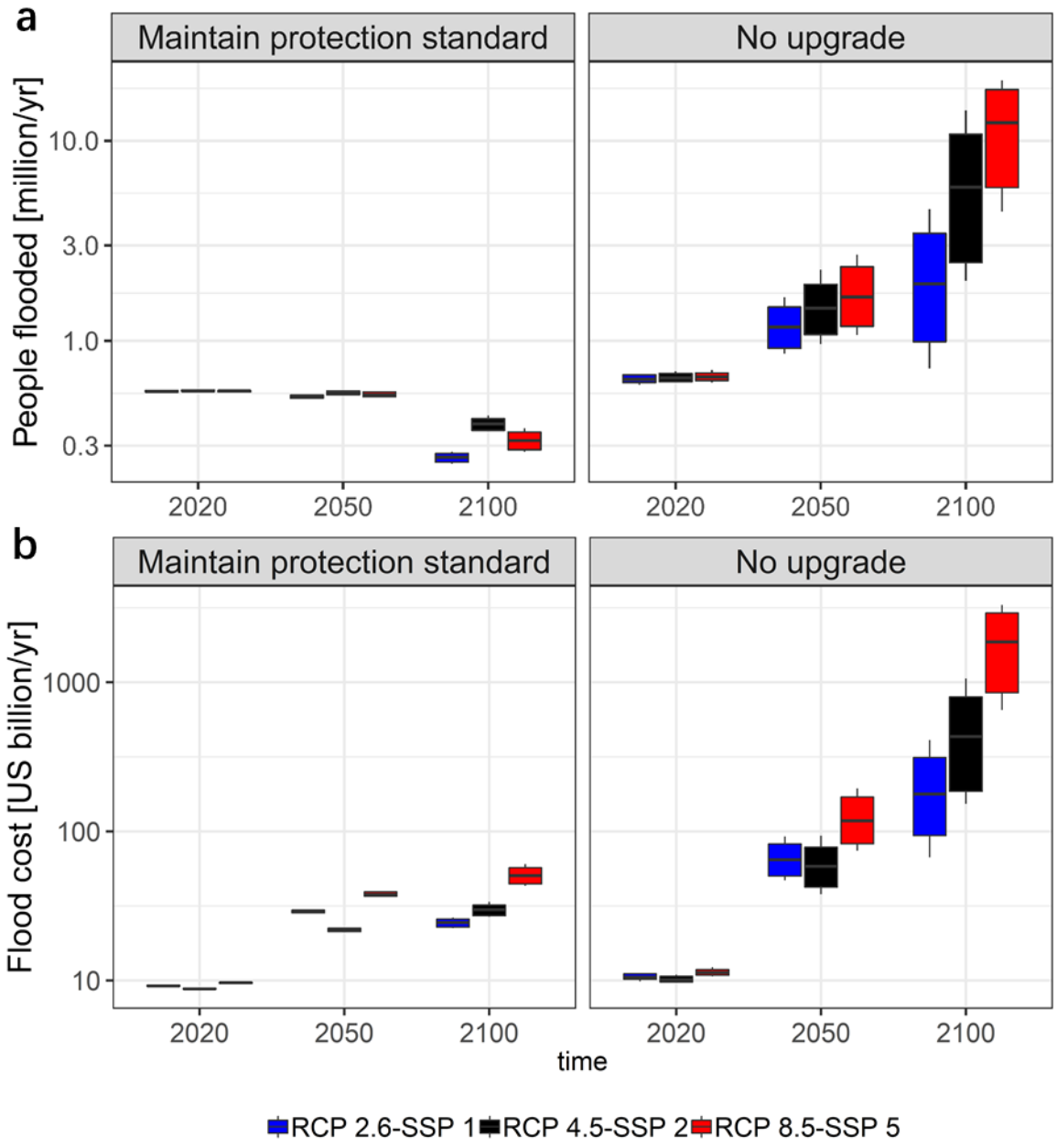

458

459 Fig. 8 People flooded and flood costs in 2020, 2050 and 2100 under two adaptation strategies.
460 On each box, the central mark indicates the median, and the bottom and top edges of the box
461 indicate the 25th and 75th percentiles, respectively. The whiskers extend to the most extreme
462 (maximum and minimum) data points.

463

464 We investigated dike costs under two adaptation strategies. If there is no upgrade of protection
465 and the dike that was built in 2010 with costs of US$ 644 billion, then there are no additional
466 capital costs for building and upgrading dikes but only costs for maintenance of existing dikes.
467 With rise of sea-level, parts of dikes are no longer effective, thus dike costs decrease with SLR

under no upgrade. Under maintaining protection standards, dikes remain effective, dike costs range from US$ 8-10 billion per year under RCP2.6-SSP1 to US$ 11-17 billion under RCP8.5-SSP5 in 2100 (Tab. 3). Comparing flood costs and dike costs, increased dike costs are two orders of magnitude smaller than reduced flood costs across all scenarios, even without accounting for indirect damages.

Tab. 3 Dike and flood costs in 2100 under multiple scenarios. The median and, in parentheses, the maximum and minimum values are provided. In the last two columns, the median value is considered to calculate reduced flood costs and increased dike costs.

RCP-SSP	Flood costs (US$billion/yr)		Dike costs (US$billion/yr)		Reduced flood costs	Increased dike costs
	No upgrade	Maintain protection standard	No upgrade	Maintain protection standard		
RCP2.6-SSP1	210 (67, 410)	24 (22, 26)	6 (4, 7)	9 (8, 10)	186 (45, 383)	3 (1, 6)
RCP4.5-SSP2	521 (153, 1060)	30 (28, 34)	4 (2, 6)	10 (9, 12)	491 (126, 1026)	6 (3, 10)
RCP8.5-SSP5	1916 (650, 3308)	51 (43, 60)	2 (0.1, 5)	14 (11, 17)	1865 (607, 3248)	12 (6, 17)

3.4 Implications

This study quantitatively assesses people effect by sea-level rise, plus flood damage and adaptation costs for coastal China using the DIVA modelling framework and considering three RCP and SSP combinations and two adaptation strategies. The results show that coastal flood risk highly depends on change in population and coastal adaptation. Sustainable development (RCP2.6-SSP1) would at least halve the damages or reduce by one order of magnitude the flood costs compared to a moderate development (RCP4.5-SSP2) or a fossil-fuel based development scenario (RCP8.5-SSP5). The intensification of ESLs with global warming is the main contributor of the increasing coastal flood risk in China. From a strategic planning perspective, coastal hard engineering protection is very effective in protecting coasts. The

488 expense of protection (dike costs) is much smaller than reduced flood damage, not to mention
489 indirect damages (e.g. damages caused by failure of coastal infrastructure network) which have
490 not been assessed here. The methods and findings can be used to provide basic information to
491 governments, policy-makers, insurance companies and local communities on the overall risk
492 at a national scale and pinpoint hotspots within coastal China for further more detailed analysis.

493 Few studies have assessed the potential costs of adaptation to coastal flood risks in China, yet
494 such estimates and subsequent actions remain a huge challenge due to the uncertainties of
495 future ESLs, variation of adaptation strategies, and socio-economic settings. Many other
496 drivers influence impacts that cannot be fully accounted in models due to the quality and the
497 lack of available datasets and constraints of computer simulation of coastal behaviours at a
498 large scale. Additionally, the datasets may not address recent policy advancements. For
499 instance, China has scrapped the one-child policy, which has not been considered in SSPs
500 (Jiang et al., 2017), which will probably increase the population exposure to flooding. We also
501 assume homogeneous population change in national scale, without considering urbanisation,
502 urbans sprawl and coastal mitigation (Merkens et al., 2018). Considering domestic migration
503 and urbanisation, coastal China attracts more population than inland areas, leading to a higher
504 population exposed to coastal flooding. Second, during the segmentation, we visually
505 interpreted remote sensing images, which encompasses to a certain degree of subjectivity. This
506 could be improved by working with local authorities and carrying out field investigations to
507 validate this dataset. Meanwhile, China's coast is highly dynamic due to intensive human and
508 economic activities (e.g coastal reclamation), which the current simulation is not able to model.
509 Segmentation and reclassification may usefully be repeated in five or ten years' time, drawing
510 on automated methods that are presently being derived (Luijendijk et al., 2018). Evidence
511 indicates that fatalities from storm surges are decreasing in China as communities are becoming
512 more resilient against coastal flooding by strengthening institutional arrangements, adaptation

and mitigation actions (Fang et al., 2017). Hence, future flood risk could be lower than estimates presented here. Moreover, we used simplified assumptions, such as stationary storm systems, and linear superposition of relative sea level rise and surge. Cyclones are for instance, underrepresented in the GTSR dataset used (Muis et al., 2016). Additionally, waves are not considered due to data availability. Cyclones may intensify with climate change, thus further rising extreme sea levels (including surge and waves) during storm conditions (Wahl et al., 2017; Vousdoukas et al., 2018). The contribution of SLR to coastal flood risk will probably increase beyond 2100 considering the lagged effects of the deep ocean and contribution of Antarctic ice sheet (Deconto and Pollard, 2016) meaning long-term adaptation is essential. Coastal flooding may be compounded by other sources such as extreme precipitation and river discharge, leading to worse impacts (Wahl et al., 2015). Lastly, human-induced subsidence due to ground fluid depletion has not been included due to lack of consistent data, even though it is widely observed and has caused large damages along coastal China (Xue et al., 2005), especially in the large cities (e.g. Shanghai and Tianjin). Subsidence will exacerbate the impacts of SLR and requires further investigations in a Chinse context.

Presently, hard engineering of building and enhancing dikes and seawalls are still the main form of adaptation measure. Hardening coasts threatens coastal biodiversity and ecosystems (Ma et al., 2014). Simultaneously, soft engineering approaches, which put more emphasis on the natural environment, such as mangrove afforestation, wetland creation, and/or combined engineering structures, such as seawall with wetland creation/beach nourishment, have become increasingly popular in recent years (Luo et al., 2015). To protect coastlines against extreme conditions coastal communities could reinforce current adaptation approaches, encourage the uptake and harness of new adaptation approaches, such as hybrid adaptation. Thus, a more comprehensive analyses of coastal adaptation options for China is required.

4 Conclusion

This study provides a quantitative risk assessment for coastal flood at national level by applying the Dynamic Interactive Vulnerability Assessment (DIVA) model in China. A high-resolution DIVA-China database for coastal China including coastal protection level information has been built to improve the assessment. Compared with the global dataset, it provides a more realistic spatial representation of coastal flood impacts for China, with a 136% increase of coastline length from 12,288 km to 28,966 km. Artificial coasts comprise more than 50% of total coastline length in China, which indicates the necessity of considering protection in the impact assessment.

Taking into account data and scenario uncertainties, the 100-year floodplain area covers an extent of 53,000 to 74,000 km^2 with 18.1-27.0 million exposed population and US$ 4.5-11.1 trillion exposed assets with 21-119 cm of relative SLR in China in 2100. In terms of risk, there are 0.7-20.0 million people expected to be flooded annually in 2100 assuming no upgrade to adaptation, and US$ 67-3,308 billion assets are at risk per year assuming no upgrade of protection compared with 2100. In contrast, maintaining current protection level, reduce protected impacts to 0.2-0.4 million people/yr and US$ 22-60 billion/yr flood costs by 2100, at only US$ 8-17 billion/yr of dike costs. Increased dike costs are two orders of magnitude smaller than reduced flood costs across all scenarios, even without accounting for indirect damages.

This research will be helpful to governments, policy-makers, insurance companies and local communities in China to provide information for designing strategies to adapt to increasing coastal flood risk. In particular, it can be updated and improved if there are better quality regional datasets available and modification of model algorithms/assumptions, to provide consistent, comparable and rapid coastal flood risk assessments for stakeholder needs.

Acknowledgements

This work is funded by the National Key R & D Program of China (2017YFE0100700; 2016YFA0602404; 2017YFC1503001); Shanghai Sailing Program (19YF1413700); China Postdoctoral Science Foundation (No. 2019M651429); European Union's Seventh Programme for Research, Technological Development and Demonstration under grant agreement No. 603396 (RISES-AM project); Special thanks to China Scholarship Council.

References

[1] Aerts, J., Major, D.C., Bowman, M.J., et al. 2009. Connecting delta cities: coastal cities, flood risk management and adaptation to climate change. VU University Press.
[2] Bright, E. A., et al. 2011. LandScan 2010. Oak Ridge, TN, Oak Ridge National Laboratory.
[3] Courtya, L.G., Soriano-Monzalvoa, J.C., and Pedrozo-Acuñaa, A. 2017. Evaluation of open-access global digital elevation models (AW3D30, SRTM and ASTER) for flood modelling purposes.
[4] Fang, J., Liu, W., Yang, S., et al. 2017. Spatial-temporal changes of coastal and marine disasters risks and impacts in Mainland China. Ocean Coast. Manag. 139, 125-140.
[5] Fu, Y.B., Cao, K., Wang, F., and Zhang, F.S., 2010. Primary quantitative evaluation method on sea enclosing and land reclamation strength and potential. Ocean Dev. Manag. 1, 27-30. (in Chinese)
[6] DeConto, R.M., and Pollard, D. 2016. Contribution of Antarctica to past and future sea-level rise. Nature 531(7596):591-597.
[7] Gao, Y, Wang, H., Su, F., et al. 2013. Spatial and temporal of continental coastline of China in recent three decades. Acta Oceanol. Sin. 35(06), 31-42. (in Chinese)
[8] Hallegatte, S., Green, C., Nicholls, R.J., et al. 2013. Future flood losses in major coastal cities. Nat. Clim. Change 3(9), 802-806.
[9] Han, M., Hou, J., and Wu, L. 1995. Potential impacts of sea-level rise on China's coastal environment and cities: A national assessment. J. Coastal Res. 79-95.
[10] Hanson, S., Nicholls, R.J., Ranger, N., et al. 2011. A global ranking of port cities with high exposure to climate extremes. Clim. Change 104(1), 89-111.
[11] Hinkel, J. and Klein, R.J., 2009. Integrating knowledge to assess coastal vulnerability to sea-level rise: The development of the DIVA tool. Glob. Environ. Change 19(3), 384-395.
[12] Hinkel, J., Lincke, D., Vafeidis, A.T., Perrette, M., Nicholls, R.J., Tol, R.S., Marzeion, B., Fettweis, X., Ionescu, C. and Levermann, A., 2014. Coastal flood damage and adaptation costs under 21st century sea-level rise. Proc. Natl. Acad. Sci. U. S. A. 111(9), 3292-3297.
[13] Hou, X., Wu, T., Hou, W., Chen, Q., Wang, Y. and Yu, L. 2016. Characteristics of coastline changes in mainland China since the early 1940s. Sci. China: Earth Sci. 59(9), 1791-1802.
[14] Hu, P., Zhang, Q., Shi, P., Chen, B. and Fang, J., 2018. Flood-induced mortality across the globe: Spatiotemporal pattern and influencing factors. Sci. Total Environ. 643, pp.171-182.
[15] Hu, Z., Peng, J., Hou, Y. and Shan, J., 2017. Evaluation of Recently Released Open Global Digital Elevation Models of Hubei, China. Remote Sens. 9(3), 262.
[16] Huang, Q., He, C., Gao, B., et al. 2015. Detecting the 20 year city-size dynamics in China with a rank clock approach and DMSP/OLS nighttime data, Landsc. Urban Plan. 137: 138-148.
[17] Huang, Z., Zong, Y., and Zhang, W. 2004. Coastal inundation due to sea level rise in the Pearl River Delta, China. Nat. Hazards 33(2), 247-264.
[18] International Institute for Applied Systems Analysis. 2012. Shared Socioeconomic Pathways Database. Available at https://secure.iiasa.ac.at/web-apps/ene/SspDb.

606 [19] Jiang, T., Zhao, J., Jing, C., et al. 2017. National and provincial population projected to 2100
607 under the shared socioeconomic pathways in China. Adv Climate Change Res. 13(02), 128-137.
608 (in Chinese)
609 [20] Jones, B., O'Neill, B.C., McDaniel, L., McGinnis, S., Mearns, L.O. and Tebaldi, C., 2015. Future
610 population exposure to US heat extremes. Nat. Clim. Change 5(7), 652.
611 [21] Kang, L., Ma, L., and Liu, Y. 2016. Evaluation of farmland losses from sea level rise and storm
612 surges in the Pearl River Delta region under global climate change. J. Geogr. Sci.. 26(4), 439-456.
613 [22] Ke Q.2014. Flood risk analysis for metropolitan areas -a case study for Shanghai[D]. TU Delft,
614 Delft University of Technology.
615 [23] Kebede, A.S., and Nicholls, R.J. 2012. Exposure and vulnerability to climate extremes:
616 population and asset exposure to coastal flooding in Dar es Salaam, Tanzania. Reg. Envir.
617 Chang. 12(1), 81-94.
618 [24] Leimbach, M., Kriegler, E., Roming, N., and Schwanitz, J. 2017. Future growth patterns of world
619 regions – A GDP scenario approach. Glob. Environ. Change. 42, 215–225.
620 [25] Li, W., Wang, J., and Chen, L. 2003. Study on storm surge protection standard of seawall
621 engineering. Water Resource Planning. Des 4:5–9. (in Chinese)
622 [26] Li, X., Rowley, R. J., and Kostelnick, J. C. 2009. GIS Analysis of Global Impacts from Sea Level
623 Rise. Photogramm. Eng. Remote Sens.75(7), 807-818.
624 [27] Liao, X., Xu, W., Zhang, J., Li, Y. and Tian, Y., 2019. Global exposure to rainstorms and the
625 contribution rates of climate change and population change. Sci. Total Environ. 663, pp.644-653.
626 [28] Liu, C. 2014. Reflections on Maritime Partnership: Building the 21st Century Maritime Silk
627 Road. China Institute of International Studies.
628 [29] Liu, J., Wen, J., Huang, Y., et al. 2015. Human settlement and regional development in the
629 context of climate change: a spatial analysis of low elevation coastal zones in China. Mitig.
630 Adapt. Strateg. Glob. Chang. 20(4), 527-546.
631 [30] Luijendijk, A., Hagenaars, G., Ranasinghe, R., Baart, F., Donchyts, G. and Aarninkhof, S., 2018.
632 The state of the world's beaches. Sci. Rep. 8(1), 6641.
633 [31] Luo, S., Cai, F., Liu, H., et al. 2015. Adaptive measures adopted for risk reduction of coastal
634 erosion in the People's Republic of China. Ocean Coast. Manag. 103, 134-145.
635 [32] Ma, Z., Melville, D.S., Liu, J., et al. 2014. Rethinking China's new great wall. Science
636 346(6212), 912-914.
637 [33] McFadden, L., Nicholls, R.J., Vafeidis, A. and Tol, R.S., 2007. A methodology for modeling
638 coastal space for global assessment. J. Coast. Res. 911-920.
639 [34] McGranahan, G., Balk, D., and Anderson, B. 2007. The rising tide: assessing the risks of climate
640 change and human settlements in low elevation coastal zones. Environ. Urban. 19(1), 17-37.
641 [35] Menéndez, M. and Woodworth, P.L., 2010. Changes in extreme high water levels based on a
642 quasi‐global tide‐gauge data set. J. Geophys. Res.: Oceans 115(C10).
643 [36] Merkens, J-L., Lincke, D., Hinkel, J., Brown, S., Vafeidis, A.T. 2018. Regionalisation of
644 population growth projections in coastal exposure analysis. Clim. Change 14(1):3.
645 [37] Messner F, et al. 2007. Evaluating flood damages: Guidance and recommendations on principles
646 and methods FLOOD-site Project Deliverable D9.1. Available at
647 http://www.floodsite.net/html/partner_area/project_docs/T09_06_01_Flood_damage_guidelines_
648 d9_1_v2_2_p44.pdf. Accessed August 26, 2019.
649 [38] Muis, S., Verlaan, M., Winsemius, H.C., Aerts, J.C. and Ward, P.J., 2016. A global reanalysis of
650 storm surges and extreme sea levels. Nat. Commun. 7.
651 [39] Nicholls, R.J. 2004. Coastal flooding and wetland loss in the 21st century: changes under the
652 SRES climate and socio-economic scenarios. Glob. Environ. Change 14(1), 69-86.
653 [40] Nicholls, R.J., Wong, P.P., Burkett, V., Woodroffe, C. D., and Hay, J. 2008. Climate change and
654 coastal vulnerability assessment: scenarios for integrated assessment. Sustain. Sci. 3(1), 89-102.
655 [41] Nicholls, R.J., Hanson, S.E., Lowe, J.A., Warrick, R.A., Lu, X. and Long, A.J., 2014. Sea‐level
656 scenarios for evaluating coastal impacts. Wiley Interdiscip. Rev.-Clim. Chang. 5(1), 129-150.

[42] Neumann, B., Vafeidis, A. T., Zimmermann, J., and Nicholls, R.J. 2015. Future coastal population growth and exposure to sea-level rise and coastal flooding - a global assessment. Plos One, 10(3), e0131375.
[43] O'Neill, B.C., Kriegler, E., Riahi, K., et al. 2014. A new scenario framework for climate change research: the concept of shared socioeconomic pathways. Clim. Change 122(3), 387-400.
[44] Peltier, W.R., 2000. Glacial isostatic adjustment corrections. In: Douglas, B.C; Kearney, M.S., and Leatherman, S.P. (eds.), Sea level rise: History and consequences. San Diego, California: Academic Press, 65-95.
[45] Samir, K.C. and Lutz, W., 2014. Demographic scenarios by age, sex and education corresponding to the SSP narratives. Popul. Env. 35(3), pp.243-260.
[46] Samir, K.C. and Lutz, W., 2017. The human core of the shared socioeconomic pathways: Population scenarios by age, sex and level of education for all countries to 2100. Glob. Environ. Change 42, 181-192.
[47] Seto, K.C. 2011. Exploring the dynamics of migration to mega-delta cities in Asia and Africa: Contemporary drivers and future scenarios. Glob. Environ, Change 21, S94-S107.
[48] Standard for Flood Control. (National Standard of the People's Republic of China.GB 50201-2014) [S]. 2014. Ministry of Housing and Urban-Rural Development of the People's Republic of China.
[49] Sun, Z., Sun, W., Tong, C., Zeng, C., Yu, X. and Mou, X., 2015. China's coastal wetlands: Conservation history, implementation efforts, existing issues and strategies for future improvement. Environ. Int. 79, 5-41.
[50] T. Tadono, H. Nagai, H. Ishida, F. Oda, S. Naito, K. Minakawa, H. Iwamoto. 2016.l Validation of the 30 m-mesh Global Digital Surface Model Generated by ALOS PRISM, The International Archives of the Photogrammetry, Remote Sensing and Spatial Information Sciences, ISPRS, Vol. XLI-B4, pp.157-162.
[51] Vafeidis, A.T., Nicholls, R.J., McFadden, L., Tol, R.S., Hinkel, J., Spencer, T., Grashoff, P.S., Boot, G. and Klein, R.J., 2008. A new global coastal database for impact and vulnerability analysis to sea-level rise. J. Coastal Res. 917-924.
[52] Van Vuuren D.P., Carter T.R. 2014. Climate and socio-economic scenarios for climate change research and assessment: reconciling the new with the old. Clim. Change 122(3): 415-429.
[53] van Vuuren DP, Edmonds J, Kainuma M, Riahi K, Thomson A, Hibbard K, Hurtt GC, Kram T, Krey V, Lamarque J-F, Masui T, Meinshausen M, Nakicenovic N, Smith SJ, Rose SK. 2011. The representative concentration pathways: An overview. Clim. Change, 109(1-2), 5–31.
[54] Vousdoukas, M.I., Mentaschi, L., Voukouvalas, E., Bianchi, A., Dottori, F. and Feyen, L., 2018. Climatic and socioeconomic controls of future coastal flood risk in Europe. Nat. Clim. Change 8(9), p.776.
[55] Wahl, T., Haigh, I.D., Nicholls, R.J., et al. 2017. Understanding extreme sea levels for broad-scale coastal impact and adaptation analysis. Nat. Commun. 8: 16075.
[56] Wahl, T., Jain, S., Bender, J., et al. 2015. Increasing risk of compound flooding from storm surge and rainfall for major US cities. Nat. Clim. Change 5(12), 1093-1097.
[57] Wang, J., Yi, S., Li, M.Y., Wang, L., and Song, C. 2018. Effects of sea level rise, land subsidence, bathymetric change and typhoon tracks on storm flooding in the coastal areas of Shanghai. Sci. Total Environ. 621:228-234.
[58] Wang B, Chen S, Zhang K, et al. 1995. Potential impacts of sea-level rise on the Shanghai area. J. Coastal Res. 151-166.
[59] Wang W, Liu H, Li Y, et al. 2014. Development and management of land reclamation in China. Ocean Coast. Manag. 102: 415-425.
[60] Wang, Y. and Aubrey, D.G., 1987. The characteristics of the China coastline. Cont. Shelf Res. 7(4), 329-349.
[61] Wang, Y., 1980. The coast of China. Geoscience Canada, 7(3).
[62] Wolff, C., Vafeidis, A.T., Lincke, D., Marasmi, C. and Hinkel, J., 2016. Effects of Scale and Input Data on Assessing the Future Impacts of Coastal Flooding: An Application of DIVA for the Emilia-Romagna Coast. Front. Mar. Sci. 3, 41.

[63] Wolff, C., Vafeidis, A.T., Muis, S., et al. 2018.A Mediterranean coastal database for assessing the impacts of sea-level rise and associated hazards. Sci. Data 5, 180044.
[64] Wu, J., Li, N., and Shi, P. 2014. Benchmark wealth capital stock estimations across China's 344 prefectures: 1978 to 2012. China Econo. Rev. 31: 288-302.
[65] Wu, T., Hou, X. and Xu, X., 2014. Spatio-temporal characteristics of the mainland coastline utilization degree over the last 70 years in China. Ocean Coast. Manag. 98, 150-157.
[66] Xu, M., He, C., Liu, Z. and Dou, Y., 2016. How did urban land expand in China between 1992 and 2015? A multi-scale landscape analysis. PloS one, 11(5), p.e0154839.
[67] Xue, Y.Q., Zhang, Y., Ye, S.J., et al. 2005. Land subsidence in China. Environmental geology. 48(6), 713-720.
[68] Yin, J., Yin, Z., Yu, D.P. and Xu, S.Y. 2012. Vulnerability analysis for storm induced flood: a case study of Huangpu River Basin. Scientia Geographica Sinica. 32(9), 1155-1160.